

Supporting Information

Ignell et al. 10.1073/pnas.0813004106

SI Text

Generation of *dtkr*-RNAi Flies. We used an RNAi vector, Sym^UAST, which generates double-stranded RNA by simultaneous transcription of both strands. The construct was designed with 2 inversely oriented UAS sequences. To generate the *dtkr*-RNAi construct, we first used a previously produced TA clone of the *dtkr* cDNA (see ref. 1). We excised a 1.4-kb fragment from the TA-clone using *Eco*RI, and cloned it into the Sym^UAST vector. These constructs (*UAS-dtkr-GFP* and *UAS-dtkr-RNAi*) were sequenced and injected into *w*¹¹¹⁸ embryos using standard germ line transformation techniques (2). From these injections several lines of both *UAS-dtkr-GFP* and *UAS-dtkr-RNAi* were established. *UAS-dtkr-GFP(10b)* was found to display strong green fluorescence when crossed to appropriate Gal4 drivers and was used for the subsequent experiments. *UAS-dtkr-RNAi(1A)* was used for all experiments here because this strain displayed the strongest and most consistent lethal phenotype when expressed globally.

Quantitative Real-Time PCR. To test the efficiency of the *dtkr*-RNAi construct, we determined the levels of *dtkr* by quantitative real-time PCR. When the *dtkr*-RNAi was driven with the pan-neuronal driver *elav-Gal4* it induced lethality in the 1st or 2nd instar larvae. Thus, we had to use first instar larvae for measuring RNA levels after knock down. Approximately 30 first instar larvae of wild-type flies (Oregon R) and *elav-Gal4;UAS-dtkr-RNAi* larvae were tested for *dtkr* transcript levels to determine the efficiency of the RNAi. All samples were homogenized in liquid nitrogen and total RNA was extracted using the recommended protocol from the RNeasy mini kit (Qiagen). RNA was quantified by spectrophotometry and transcribed using the SuperScript II First-Strand cDNA synthesis kit (Invitrogen). Reverse transcription products were quantified using an ABI PRISM 7700 (Applied Biosystems). PCRs were set up as triplicates using SYBR Green Master Mix (Applied Biosystems). Experiments were made in 3 replicates, starting from new RNA extractions. *rp49* was used as an internal transcriptional standard. All calculations were made using software from Applied Biosystems.

Primer Sequences. Quantitative real-time PCR: Primers for *dtkr* were 5'GAGTAAGCGAAGGGTGGTGAAG and 3'GAACGCGACCCAGCAGAT, for *rp49*: 5'AGCGCACCAAGGACTTCGT and 3'GCCATTTGTGCGACAGCTT.

Semiquantitative Reverse Transcriptase PCR. Primers for *dtkr* were 5'CGGATAAAGACAAAGGAAAACACT and 5'GAATGATGAGGATGTTGTAG, primers for *dtk* were: 5'TCCGATTCTATGACTTGAGAG and 5'GCGAGGCATACGGCCAGCACTTT, primers for *rp49* were: 5'GTATCGAACACAGATCGGTCGC and 5'TTGGTGAGCGGACCGACAGCTGC.

To distinguish PCR bands amplified from cDNA from those amplified from any remaining genomic DNA, we used primer pairs that spanned introns.

Immunocytochemistry. Dissected fly brains were fixed in PBS containing 4% paraformaldehyde and 1.0% Triton X-100 (PBS-T) for 2–4 h on ice, and blocked in 2.0% normal goat serum PBS-T overnight at 4 °C. To test for the coexpression of DTK in populations of GFP-expressing neurons in *GH298-Gal4* and *Gad1-Gal4* flies, we incubated the brains with an antiserum to a generic sequence of insect tachykinin-related peptides

(anti-LemTRP-1; code K 9836) (3) at a dilution of 1:4,000 and a mouse monoclonal antibody against GFP (1:100, Molecular Probes). Bound antibodies were detected with secondary Cy3, AlexaFluor-488 or AlexaFluor-546 conjugates (Molecular Probes). To detect the ectopic expression of DTKR in the different Gal4 lines, visible through the GFP fusion construct (*UAS-dtkr-GFP*), we incubated the fixed brains in the monoclonal antibody against GFP.

DTKR immunocytochemistry was performed as described by Birse et al. (1). For detection of DTKR immunoreactivity adult fly heads were fixed for 3 h in ice-cold Bouin's fixative (picric acid:formaldehyde:glacial acetic acid, 15:5:1). After rinsing in 0.1 M phosphate buffer, heads were dehydrated in a series of alcohol/xylene. Dehydrated heads were embedded in paraffin and sectioned (9 μm). Sections were rehydrated, followed by blocking with normal goat serum for 2 h in room temperature. Incubation with primary antiserum to DTKR (1), used at 1:500 dilution, was carried out for 48 h at 4 °C. Primary antiserum was detected using Cy3-conjugated goat anti rabbit secondary antiserum diluted 1:1500 (Jackson ImmunoResearch).

Brains and sections were mounted in VectaShield (Vector Laboratories) and image stacks were collected on a Zeiss LSM 510 confocal laser-scanning microscope. For each experiment, at least 10 specimens were analyzed.

Two-Photon Microscopy. GCaMP and spH imaging were performed with a two-photon microscope, which was built from off the shelf components similar to that described in ref. 4. The upright fixed stage microscope was assembled onto an optical rail, which sits on an X-Y motorized stage (Precision Systems) controlled by a modified MP-285 driver (Sutter Instruments). A stepping motor (PK245–01AA, Oriental Motor), also controlled by the modified MP-285 driver, was used to move the objective lens (Achromplan IR 40×/0.8NA, Zeiss) in the vertical direction.

The light source was a Chameleon XR titanium:sapphire laser (Coherent). Mode-locked laser output had an ultra-short pulse width of <140 fs at a repetition rate of 90 MHz. The laser power for sample excitation was attenuated by a Pockels cell (350–80 LA-BK, Conoptics). Laser light of an ≈925-nm wavelength was used for excitation. Laser beam scanning was controlled by a pair of galvanometer 3 mm mirrors (6210, Cambridge Technology) driven by custom software CfNT (version 1.580d) kindly provided by Winfried Denk. A dichroic mirror (595DCXR) allowing the infrared laser beam to pass and reflect visible points, was placed on top of a binocular phototube (Zeiss) between the scan lens and the tube lens. A blocking filter (E700SP-special) and a band-pass filter (HQ525/50 m, for two-photon application) were inserted between the focusing lens and the PMT light detector (H7422P-40, Hamamatsu Photonics) to select for the emission spectrum of GCaMP (peak at 509). All optical filters were from Chroma Technology Corporation. Protected silver-coated mirrors (New Focus) were used for beam reflection.

Data acquisition was performed with CfNT software (version 1.580d) on a dual 2.8 GHz Pentium 4 computer, running Windows XP, and equipped with an imaging board (XPG-1000, Coreco) and a Fulcrum data acquisition board (DT3809) to interface with external devices including shutter, scanning mirrors, XYZ stepping motors, and light detectors.

Images were acquired at approximately 4 frames/s (256 ms per frame) with a resolution of 128 × 128 pixels. For each stimulation, 80 frames (≈20 s) were acquired, with a 5-s delay before stimulation onset. After all stimulations were complete, a 512 ×

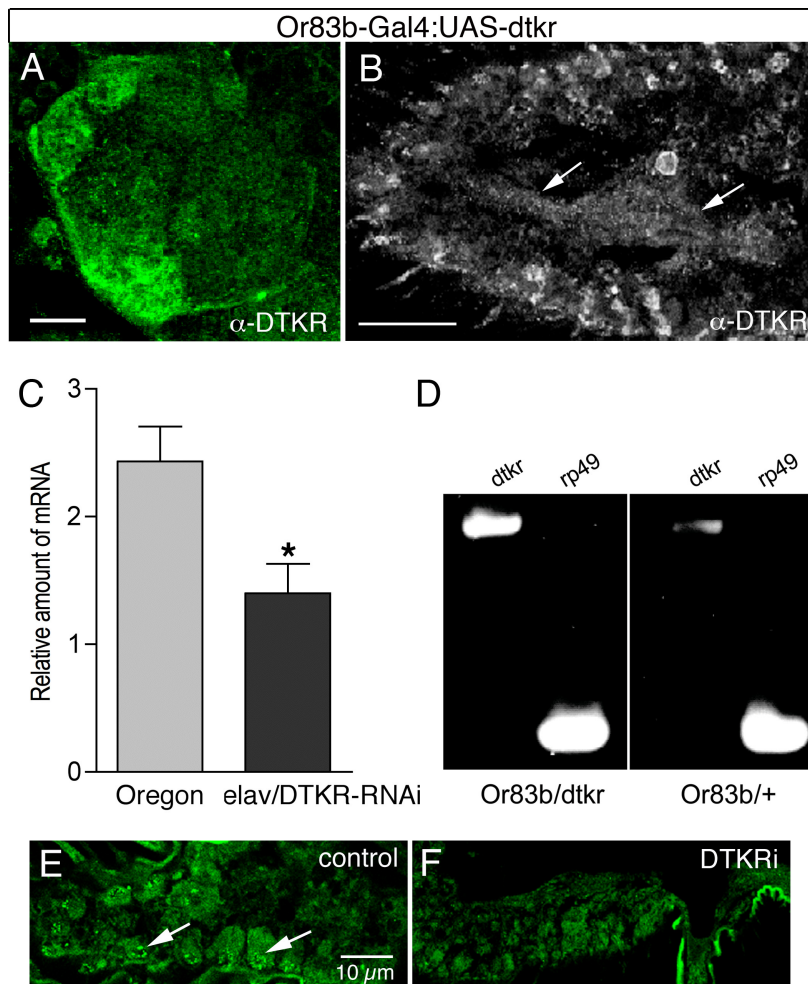


Fig. S1. Analysis of *dtkr* over-expression and RNA interference. (A and B) Using the transgenes *Or83b-Gal4* and *UAS-dtkr* we overexpressed the tachykinin receptor in ORNs. The receptor protein could now be readily detected by immunolabeling with the DTKR antiserum in the antennal lobe (A) and antenna (B). Note that with overexpression of *dtkr* in the ORNs their axons can be displayed with the DTKR antiserum (arrows in B). (C) Quantitative real-time PCR analysis of *dtkr* expression in wild-type (Oregon-R) and in *dtkr-RNAi* in first instar larvae. Transcription levels in larvae expressing *UAS-dtkr-RNAi* driven by the pan-neural *elav-Gal4* (*elav-Gal4/+;UAS-dtkr-RNAi1a/+*) are reduced by $\approx 40\%$ compared with expression levels in wild-type larvae. Transcript levels are normalized to the ribosomal protein *rp49* as an internal standard. Each bar represents the average of 3 independent RNA extractions. Student's *t* test, $P < 0.05$. (D) Reverse transcriptase PCR analysis of *dtkr* expression in isolated antennae from flies expressing *UAS-dtkr* driven by the olfactory receptor neuron *Or83b-Gal4* (*w¹¹¹⁸;Or83b-Gal4/UAS-dtkr*) and from control flies (*w¹¹¹⁸;Or83b-Gal4/+*). Increased amounts of *dtkr* PCR products in *Or83b/dtkr* compared with *Or83b/+* demonstrate that the *dtkr* construct is producing ectopic expression in antennae. Parallel reactions with *rp49* as a template control were performed. (E and F) Immunocytochemical analysis of DTKR expression in antenna of a control fly (E; *Or83b-Gal4*) and a fly expressing *dtkr-RNAi* in *Or83b-Gal4* neurons in which a reduction of DTKR protein can be seen. Two ORNs immunolabeled by DTKR antiserum are indicated by arrows in E.

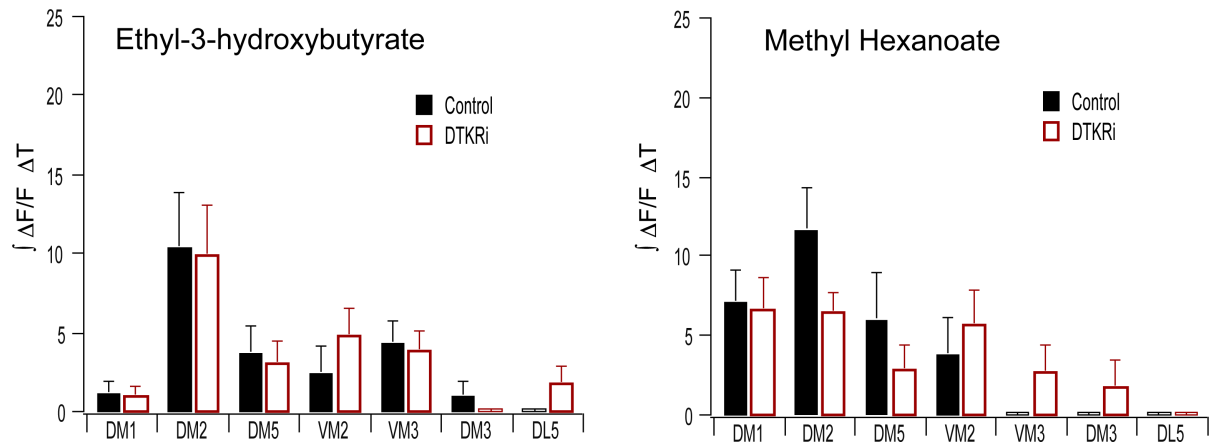


Fig. S2. Presynaptic tachykinin receptors do not affect odor-evoked response to low odor concentration. Two-photon imaging of ORN synaptic transmission elicited by odor stimulation at low odor concentration (10^{-4}) in control flies and flies expressing *dtkr-RNAi* in Or83b neurons. Odor-evoked responses for ethyl-3-hydroxybutyrate and methyl hexanoate are quantified as the integrated fluorescence change over time for each glomerulus. No significant differences (*t* test) were detected between control and *dtkr-RNAi* flies. Flies express spH in Or83b neurons. Odors were delivered for 2 s. $n = 7-8$ preparations.

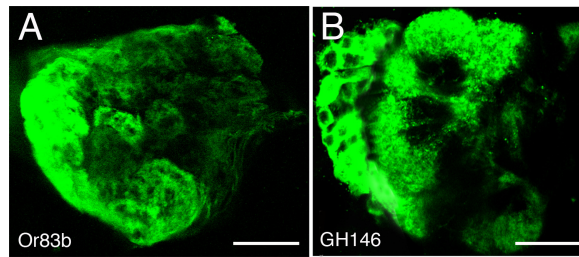


Fig. S3. Visualization of ectopic expression of the receptor DTKR. Using *UAS-dtkr-GFP* flies we could ectopically express GFP-tagged DTKR in different neurons and visualize expression pattern. (A) Ectopic expression of DTKR-GFP in a majority of the olfactory receptor neurons (ORNs) after crossing with *Or83b-Gal4*. (B) Expression in projection neurons in *GH146-Gal4* line. (Scale bars, 20 μm .)

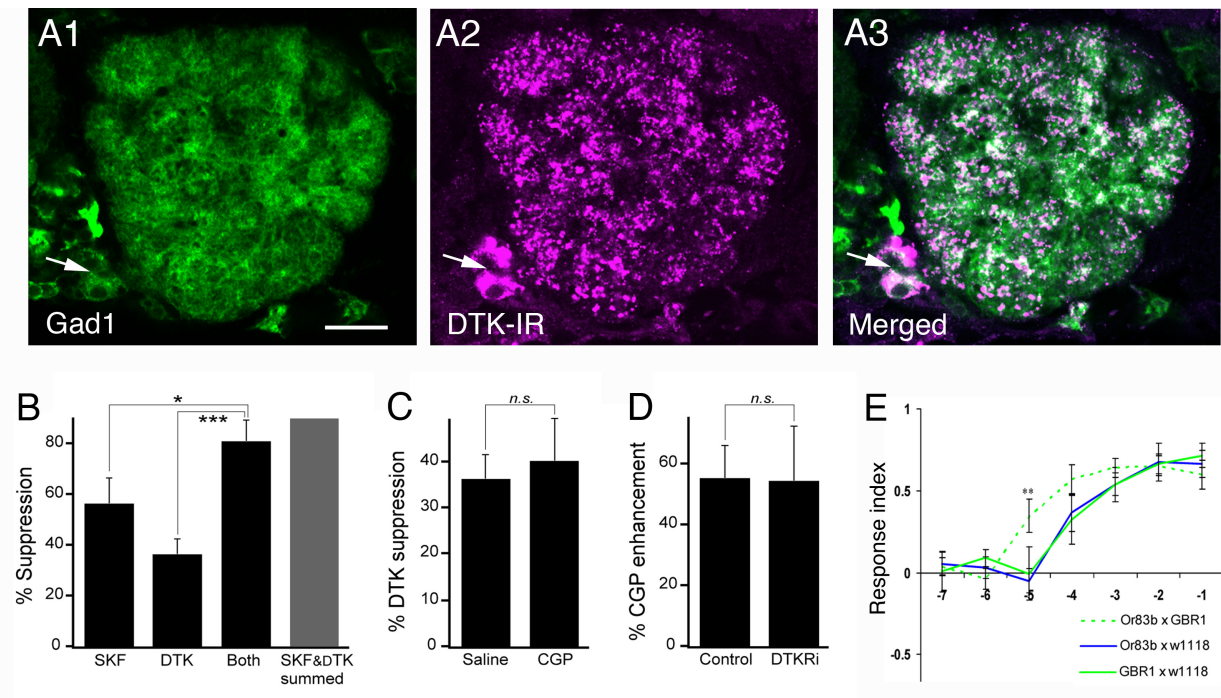


Fig. 55. Presynaptic inhibition by tachykinin receptors is independent of GABA_B receptor signaling. (A) Gad1-Gal4 is expressed in local interneurons (LNs) likely to produce GABA (A1). DTK immunoreactivity (DTK-IR) is seen in LNs (arrows) with processes in most, if not all, glomeruli (A2). When merging the images it is clear that some LNs (arrow) in this cryostat section colocalize DTKs and Gad1-driven GFP (A3). (B–D) Two-photon imaging of ORN calcium or synaptic transmission was used to monitor DTKR and GABA_BR modulation of the presynaptic response to electrical stimulation of the olfactory nerve. (B) Suppression of presynaptic calcium activity by application of the GABA_B agonist SKF97541 (SKF) (9, 10), DTK or both. The gray bar (Right) shows the quantitative summation of the SKF and the TK effect. The effect does not appear to be synergistic. (C) Blocking GABA_BR does not alter the DTK-mediated suppression of presynaptic calcium. DTK was added in saline or in the presence of the GABA_BR antagonist CGP54626 (CGP) (9–11). (D) Blocking GABA_BR with CGP enhances synaptic transmission from ORNs in control flies and flies that also express *dtkr-RNAi* in ORNs. Flies express GCaMP (A and B) or spH (C) in Or83b neurons. Suppression and enhancement are calculated by comparing the response before and after drug addition, and the values are given as the percent decrease or increase in integrated $\Delta F/F$. Electrical stimulations were 1 ms in duration and 10 V in amplitude, 45 pulses (B and C) or 80 pulses (D) at 100 Hz. *n*, 8 (B), 5–8 (C) and 5–13 (D). *t* test: *, $P \leq 0.05$; ***, $P \leq 0.001$, *n.s.* $P \leq 0.75$. (E) Olfactory choice behavior of flies with GABA_B receptor expression reduced by GABA_BR2-RNAi in ORNs (Or83b). The response to ethyl-3-hydroxybutyrate is affected at 10^{-5} displaying an increased response index. ANOVA, Tukey's posttest: **, $P < 0.01$.